American Mineralogist, Volume 61, pages 788–803, 1976

Geophysical constraints on radial and lateral temperature variations in the upper mantle

SEAN C. SOLOMON

Department of Earth and Planetary Sciences
Massachusetts Institute of Technology
Cambridge, Massachusetts 02139

Abstract

Temperatures in the upper mantle may be inferred from measurements of physical properties which are strongly dependent on temperature and by identification of seismic discontinuities with phase transitions of measurable equilibrium boundaries. Temperature at the top of the low-velocity zone, equated with the onset of incipient melting, is generally 1100° ± 100°C from a wide variety of evidence. The extensive melting detectable beneath mid-ocean ridges implies temperatures above 1250°C in the shallow asthenosphere under spreading centers. Below a thermal boundary layer at the top of the asthenosphere, associated with convection on a scale secondary to plate motions, geotherms in the asthenosphere follow nearly adiabatic gradients and intersect the olivine–spinel transition at a temperature of 1300° ± 150° C. The olivine–spinel transition is elevated about 100 km in subducted oceanic lithosphere, implying a 1000°C temperature contrast between slab and normal mantle at 250 km depth. Systematic thermal differences between stable ocean basins and continental shields are necessary but are not likely to extend deeper than 200 km. Lateral temperature variations of perhaps 200°C do persist deeper than 200 km and are probably associated with convective flow in the asthenosphere.

Introduction

The temperature distribution in the earth is intimately related to the dynamics of its interior and is fundamental to a proper interpretation of much of the data from solid-earth geophysics, geochemistry, and petrology. Direct observation of the temperature distribution is limited to measurement of temperature and its spatial derivatives in the upper few kilometers of the earth's crust. This paper is a synthesis of the many indirect observations, mostly geophysical, that provide information on the radial and lateral variations of temperature in the upper mantle.

Temperatures in the upper mantle may be estimated using two types of inference chains: (1) the identification of seismic discontinuities with phase transitions whose equilibrium boundaries can be measured in the laboratory, and (2) the measurement of physical properties which are strongly dependent on temperature. The first class of constraints includes the location of the boundaries of the low-velocity zone, interpreted as the onset of partial melting, and of the discontinuities marking the breakdown of the olivine and spinel phases of $(Mg,Fe)_2SiO_4$. The second class includes information on the depth dependence of thermally-activated properties such as electrical conductivity, seismic dissipation, and viscosity.

Both types of constraints are brought together in this paper to develop a self-consistent picture of upper mantle temperatures. The picture is closely related to recent ideas about the structure and evolution of the lithosphere and the convective flow pattern within the asthenosphere.

Phase boundaries as geothermometers: the low-velocity zone

The seismic low-velocity, low-Q zone has traditionally been identified by seismologists and others as the asthenosphere (*e.g.*, Press, 1959). The top of the low-velocity zone probably marks the locus of the solidus of mantle material in the presence of small amounts of a free fluid phase (Kushiro *et al.*, 1968; Lambert and Wyllie, 1968; Ringwood, 1969), and thus constitutes a geothermometer if the phase diagram for mantle material is assumed to be known. Variations in the depth to the top of the low-velocity zone represent lateral differences in temperature and perhaps composition.

Evidence for incipient melting

Several lines of evidence support the hypothesis that the low-velocity zone is generally in a state of incipient melting, a term proposed by Ringwood (1969) to distinguish the small amount (~1%) of melting associated with the lowering of the solidus by free H_2O or CO_2 from the greater amount of melting (5–30%) thought necessary to produce most basaltic magmas:

(1) The detailed distributions of velocity and Q of P and S waves in the upper mantle require that some sort of shear-relaxation process operate in the low-velocity zone. The rationale for this conclusion has been summarized by Anderson and Sammis (1970) and by Solomon (1972), and includes the following: the sharp gradients in velocity and Q^{-1} at the top and bottom of the zone, the much larger variation in modulus and in losses for shear than for compression, and the apparent frequency dependence of Q^{-1} in the upper mantle. A small amount of partial melting within the low velocity zone can readily account for these observations (Walsh, 1969).

(2) The temperature at the base of the lithosphere is in excess of the solidus for peridotite with small amounts of H_2O or CO_2 (Wyllie, 1971; Green, 1973b; Mysen and Boettcher, 1975). The data used to establish this result are discussed in a later section.

(3) There are numerous geochemical and petrological grounds favoring some H_2O and CO_2 in the mantle at asthenosphere depths. These include hydrous minerals in ultramafic nodules and other rocks believed to be derived from the mantle (Oxburgh, 1964; Kushiro *et al.*, 1967; McGetchin *et al.*, 1970; Merrill *et al.*, 1972), CO_2-filled inclusions in olivine-bearing nodules thought to be mantle-derived (Roedder, 1965); the presence of and oxidation state of gases given off during volcanic eruptions (Eaton and Murata, 1960; Holland, 1962; Nordlie, 1971), the mechanism of emplacement of diatremes (Shoemaker *et al.*, 1962; McGetchin and Silver, 1972), the vesicularity of young basalts erupted on the ocean floor (Moore, 1970), and the experimental melting relations for certain types of basalts (Bultitude and Green, 1967; Green, 1973a).

It is expected that any H_2O in the mantle would be present as a free fluid phase or dissolved in a silicate melt below the depth in the mantle at which amphibole and perhaps phlogopite are stable phases (Kushiro *et al.*, 1968; Lambert and Wyllie, 1968). Such an expectation is consistent with the depth to the low-velocity zone and with independent estimates of temperature at that depth (see below). Whether CO_2 would be concentrated in a fluid or a solid phase at mantle depths appropriate to the low velocity zone is a matter of some uncertainty (Green, 1972; Irving and Wyllie, 1973; Newton and Sharp, 1975), though as long as *some* H_2O is present then this uncertainty does not affect the discussion here.

The oceanic lithosphere

Thermal models for the oceanic lithosphere, together with experimentally determined phase relationships for probable mantle compositions, predict that the solidus deepens with lithospheric age (Wyllie, 1971; Forsyth and Press, 1971). The depth to the top of the low-velocity zone beneath oceans, interpreted as the depth to the solidus, can be located by several different seismic techniques and appears to deepen systematically with sea-floor age in the manner proposed (Leeds *et al.*, 1974; Forsyth, 1975).

The occurrence of a low-velocity zone is normally demonstrated in a refraction experiment by a time offset in the travel time versus distance curve for first arrivals and/or a distance range over which first-arriving signals have low amplitudes, and in a surface-wave experiment by direct inversion of surface-wave phase or group velocities. For both types of experiments, there is a trade-off between the depth extent of the low-velocity zone and the velocity within the zone. The bottoms of low-velocity zones are therefore never located with much reliability. The top of a low-velocity zone (for P waves) can often be reasonably well located by a refraction experiment, but for inversion of surface-wave dispersion there is usually another trade-off between (S wave) velocity in the lid above the low-velocity zone and depth to the top of the zone. If the lid velocities are themselves lower than normal, as in many tectonic areas, there is an additional ambiguity in choosing where the lid stops and the low-velocity zone begins.

A summary of estimates of lithospheric thickness, as defined by the depth to the low-velocity zone, beneath oceans is given in Figure 1. The most extensive data come from surface-wave phase velocities "regionalized" into zones of different ages (Leeds *et al.*, 1974; Weidner, 1974; Forsyth, 1975). Disagreement among the different determinations do not necessarily imply different thickness-age relations among the several oceans sampled, but more likely represent the sensitivity of the estimated lithosphere thickness to assumptions made in the inversion. Seismic refraction experiments at ridge crests (Francis and Porter, 1973; Orcutt *et al.*, 1975) and in older oceanic lithosphere (Asada and Shimamura, 1975)

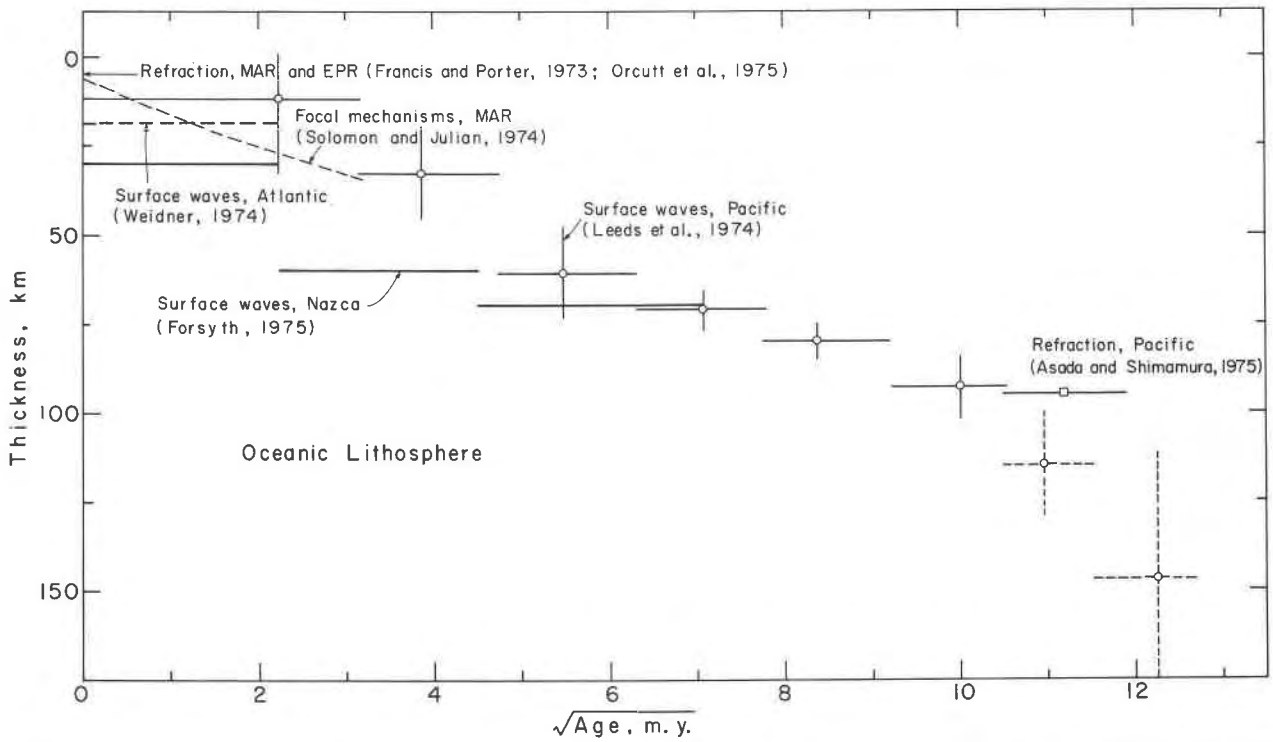

FIG. 1. Seismic determinations of oceanic lithosphere thickness, equated with the depth below sea level to the top of the low-velocity zone. Estimates from inversion of surface-wave phase velocities for various sea-floor age intervals are from Leeds *et al.* (1974) for the Pacific, Weidner (1974) for the Atlantic, and Forsyth (1975) for the Nazca plate. Ridge-crest refraction experiments by Francis and Porter (1973) on the mid-Atlantic ridge and Orcutt *et al.* (1975) on the East Pacific Rise found the top of the asthenosphere within the oceanic crust. The long refraction line of Asada and Shimamura (1975) was in the western Pacific basin east of Honshu. The dashed curve is from the ridge model of Solomon and Julian (1974) fitted to distortions in the propagation directions of teleseismic *P* waves from ridge-crest earthquakes.

lend confidence to the general trend displayed by the surface wave results, except for the results of Leeds *et al.* (1974) on sea floor older than 100 m.y., since revised (Leeds, 1975) and in much better agreement with refraction results. The implications of Figure 1 for temperature in the oceanic upper mantle are discussed below.

The continental lithosphere

Seismic data on the thickness of the continental lithosphere are more abundant than for oceanic regions, but cannot be neatly categorized as monotonic functions of only one parameter. Reliable determinations of depth to the continental low-velocity zone are summarized in Figure 2, with the results grouped roughly (after Knopoff, 1972) into tectonically active regions, stable continental platforms, and Precambrian shields. The great majority of the data come from North American profiles.

The thicknesses shown for tectonically active areas are all from the western United States, though portions of east Africa appear to be similar (Knopoff, 1972). Such regions are characterized by very pronounced low-velocity zones extending upward to shallow mantle depths, sometimes to the base of the crust. Refraction profiles give lithosphere thicknesses of 30 to 70 km for such regions, a result generally supported by inversion of phase velocity (Biswas and Knopoff, 1974) and Q^{-1} (Lee and Solomon, 1975) for Love and Rayleigh waves over similar paths.

The aseismic continental platforms, typified by midwestern North America but also including large portions of most continents (Knopoff, 1972), are characterized by a definite low-velocity zone, but one that is deeper and less pronounced than in areas of recent tectonic activity. Lithospheric thicknesses lie in the range 80 to 140 km, with perhaps 120 km a good representative figure (Biswas and Knopoff, 1974; Lee and Solomon, 1975).

The older shield regions have very modest low-velocity zones, if any. Surface-wave dispersion and some refraction profiles in shields can be fitted by models with no low-velocity zones (Brune and Dorman, 1963; Knopoff, 1972; Alexander and Sherburne,

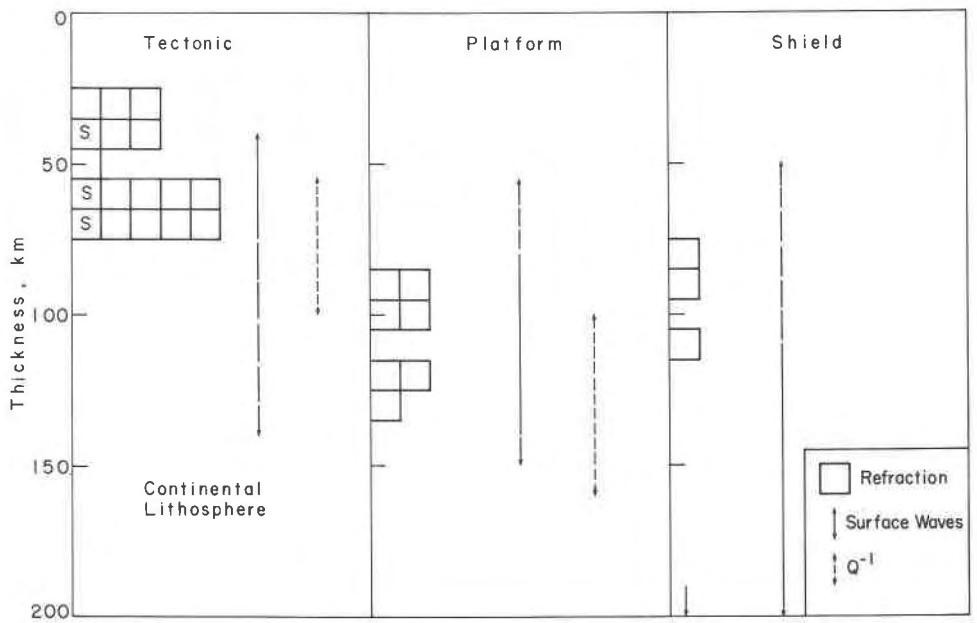

FIG. 2. Seismic determinations of continental lithosphere thickness, equated with the depth to the top of the low-velocity zone. Each box represents the thickness determined from one refraction profile; an *S* within the box designates an *S*-wave profile. The range of lithosphere thicknesses obtained from inversion of surface wave phase velocity (Knopoff, 1972; Biswas and Knopoff, 1974) and attenuation (Lee and Solomon, 1975) are shown as solid (where preferred) to long dashed and short dashed lines, respectively. Tectonic refraction profiles include CIT204 (Johnson, 1967), CIT109 through CIT112 (Archambeau *et al.*, 1969), STAN3 (Kovach and Robinson, 1969), US26 (Anderson and Julian, 1969), NTS N3, NTS NE1, and NTS E1 (Julian, 1970), SDL-UT-BR1 (Massé *et al.*, 1972), HWA and HWB (Wiggins and Helmberger, 1973), and SHR14 (Helmberger and Engen, 1974). Platform refraction profiles include ER2 (Green and Hales, 1968), NC1, YUKON4, UTAH1, NTS NE1-W. Plains, and NTS E1-W. Plains (Julian, 1970), and the Mexico profile of Shurbet (1972). Shield refraction profiles include YLKNF10 and HUDSBY10 (Julian, 1970), the Early Rise model of Massé (1973), and SMAK1 (Simpson *et al.*, 1974), the last of which found no low-velocity zone necessary (arrow at bottom of figure).

1972). For such regions the temperature profile may be everywhere subsolidus, and the usual identification of the top of the low-velocity zone as the base of the lithosphere loses its utility.

Spreading centers: the anhydrous solidus

Throughout most of the low-velocity zone the amount of melt present is likely to be small, on the order of 1 percent, and controlled by the H_2O and CO_2 abundances in the asthenosphere. The melt fraction will be appreciable (~10 percent) only when the temperature is close to the anhydrous solidus (Wyllie, 1971; Green, 1971), a condition restricted to regions of upwelling from deep within the asthenosphere such as beneath mid-ocean ridges. When the fraction of melt exceeds a few percent, the shear modulus is substantially reduced from the value for solid material or for incipient melting (Walsh, 1969). If the increase in melt fraction occurs over a narrow temperature interval reasonably well approximated by the anhydrous solidus (Wyllie, 1971), the seismic location of this melt-fraction boundary can be used as another geothermometer.

Such a melt-fraction boundary has been inferred beneath the mid-Atlantic ridge on the basis of two types of seismic measurements: very low Q for shear waves propagating through the region of extensive melting enclosed by the boundary (Solomon, 1973) and severe distortion of the propagation directions of teleseismic *P* waves from ridge-crest earthquakes because of the pronounced velocity gradients across the boundary (Solomon and Julian, 1974). The zone of extensive melting is roughly 40 to 60 km in half-width in the north Atlantic and from several km to several tens of km in thickness, in agreement with the degree of melting (~30 percent) and the magma segregation depth (15–25 km) inferred for ocean-ridge mantle from the chemistry of sea-floor basalts (Kay *et al.*, 1970). As predicted by most thermal models for spreading centers, the width of the extensively molten

zone appears to scale approximately with the spreading rate (Solomon and Julian, 1974).

Other constraints on upper mantle temperatures

The identification of the top of the low-velocity zone with the mantle solidus permits a determination of temperature at the base of the lithosphere in each of the regions mentioned above. In this section, such an exercise is combined with a number of independent techniques for estimating temperatures in the upper 100 to 200 km of the mantle to present a coherent picture of temperatures in the shallow asthenosphere. Most of the emphasis in this section will be on oceanic regions, with a discussion on continent-ocean differences reserved for later.

Figure 3 summarizes the various constraints on oceanic mantle temperatures. The locus of the solidus is sketched from Figure 1. The location of the anhydrous solidus is taken from Solomon and Julian (1974). Temperatures at various depths on both boundaries are taken from the experimental phase diagram of Green (1973b) on pyrolite plus 0.2 percent H_2O; somewhat lower temperatures would be indicated if the generally similar phase diagrams of Mysen and Boettcher (1975) or of Milhollen *et al.* (1974) on peridotite plus H_2O were employed. Other entries in the figure are discussed in turn.

Lava temperatures

Temperatures measured on erupting lavas, if no cooling process other than adiabatic decompression has operated on the lavas between magma segregation and eruption, are within perhaps 50° to 100°C of the temperature of the source of the magma beneath the point of eruption. Measured temperatures in lava fountains and lava lakes in Hawaii range between about 1060° and 1190°C (Ault *et al.*, 1961; Kinoshita *et al.*, 1969). Identifying the magma source with the base of the lithosphere beneath Hawaii (Eaton and Murata, 1960) gives a temperature at the top of the asthenosphere of 1200° ± 100°C, probably somewhat higher than beneath nonvolcanic regions.

Mineralogical geothermometers and geobarometers

The magma temperatures of several ocean-floor basalts have been calculated by Frey *et al.* (1974) with two independent techniques. Using the Kudo and Weill (1970) plagioclase thermometer as refined by Mathez (1973) to account for the non-ideal solid-solution behavior of plagioclase, Frey *et al.* obtained plagioclase crystallization temperatures on four samples of 1230 to 1250°C. Scheidegger (1973) obtained higher temperatures without the Mathez refinement. Frey *et al.* also obtained temperatures in the range 1170 to 1220°C on three samples from the olivine-liquid equilibria data of Roeder and Emslie (1970). As pointed out by Frey *et al.*, their determinations fit well with the 1 atmosphere liquidus temperatures of ridge basalts (1190° to 1250°C) measured by Tilley *et al.* (1972). These temperatures are in good agreement with magma segregation at 15 to 25 km depth (Kay *et al.*, 1970) and the temperatures indicated beneath the ridge crest in Figure 3.

Pyroxene geothermometry (Boyd, 1973) on mantle-derived ultramafic xenoliths offers considerable promise for providing estimates of the local geotherm at the time the xenoliths were brought from deep in the lithosphere or asthenosphere to near the surface. The technique is not without some uncertainties and corrections yet to be worked out (*e.g.*, Boettcher, 1974; Wilshire and Jackson, 1975), but is useful at present to corroborate other estimates of temperature.

Pyroxene geotherms for several regions designated as oceanic have been constructed by MacGregor (1974) and MacGregor and Basu (1974) and by Mercier and Carter (1975). The data most readily applied to a known oceanic environment are those from xenoliths in Hawaiian alkali basalts. The Hawaiian geotherms of both Mercier and Carter (1975) and MacGregor and Basu (1974) (the latter after shifting to 15 percent lower pressures as an approximate correction for Fe and Ca to MacGregor's (1974) geobarometer based on Al_2O_3 solubility in orthopyroxene) indicate temperatures in excess of 1100°C below about 90 km depth, in adequate agreement with other estimates.

Oceanic heat flow and topography

The variation of oceanic heat flow and bathymetry with sea-floor age is well matched by thermal models for the oceanic lithosphere based on a spreading plate with an isothermal lower boundary (McKenzie, 1967; Sleep, 1969; Sclater and Francheteau, 1970; Sclater *et al.*, 1971; Parsons and Sclater, 1975). The fit of models to observations provides constraints on both the thickness and the temperature at the base of such a plate. A recent analysis (Parsons and Sclater, 1976) of the probable values of these parameters gave 117 ± 15 km and 1560 ± 390°C, respectively. The uncertainties are probably even larger than the formal errors given, since uncertainties in several physical parameters, notably thermal conductivity, were not included. That the plate thickness determined from thermal models exceeds the depth to the low-velocity

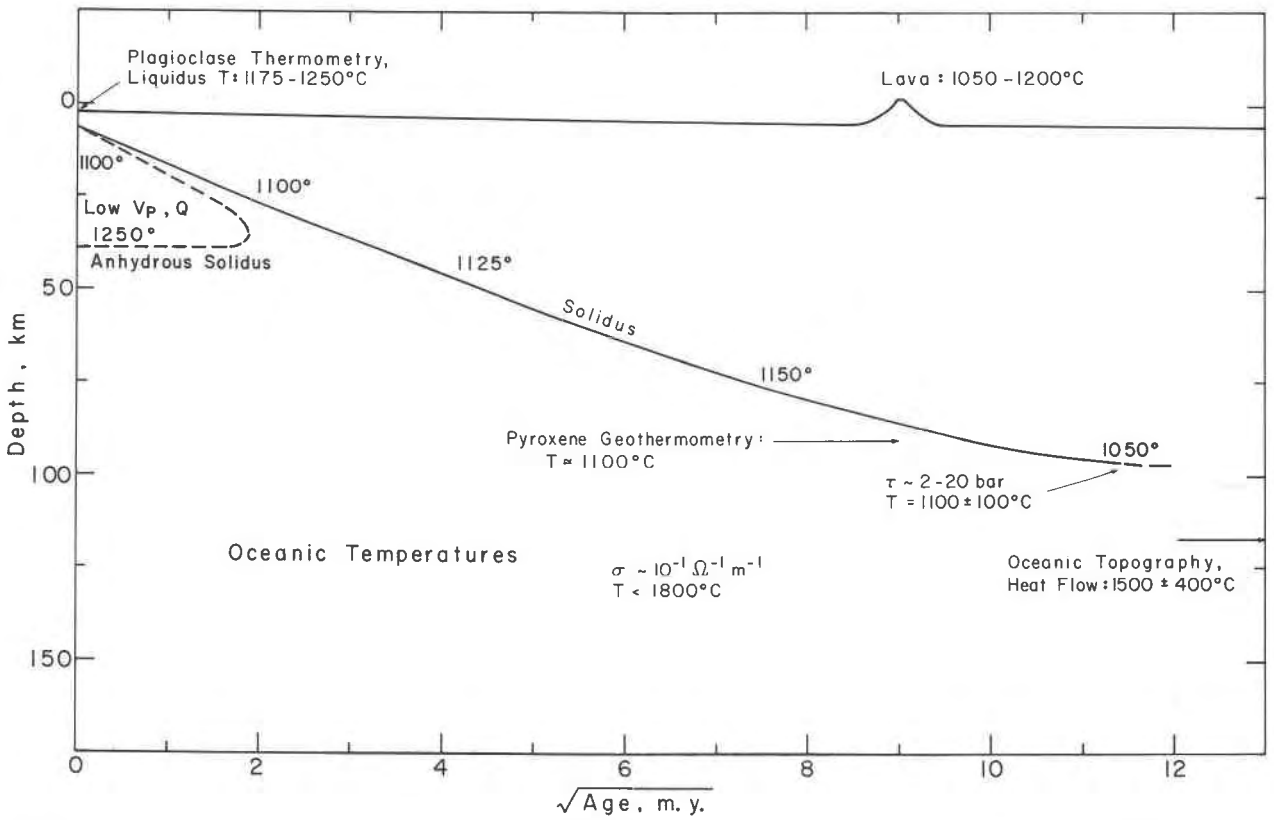

FIG. 3. Various independent estimates of temperature in the oceanic asthenosphere. Discussion of estimates and sources of data are given in the text; σ is electrical conductivity, and τ is shear stress.

zone is to be expected, since the upper part of a convective boundary layer at the top of the asthenosphere probably moves with the overlying lithosphere. The temperature at 120 km depth, which scales approximately as the heat flow in old ocean basins, is higher than most other estimates in Figure 3, but the various uncertainties overlap.

Viscosity

Viscosity is one of several physical properties that are extremely sensitive to variations in temperature. Thus, although the viscosity in the asthenosphere is very difficult to measure with much precision, even a rough estimate can be a useful constraint on temperature.

Limits on the viscous drag coefficient acting on the base of lithospheric plates have been obtained by comparing the lithospheric stress field calculated from plate tectonic driving force models (Solomon *et al.*, 1975; Richardson *et al.*, 1976) with the intraplate stress inferred from midplate earthquake mechanisms (Sykes and Sbar, 1973) and *in situ* measurements. The best fit of calculated and observed directions of principal stresses arises when viscous drag acts to retard plate motion and when the shear stress τ at the base of the lithosphere lies in the range (.001 to .01) $\sigma_R v$, where σ_R is the compressive stress near spreading centers and v is the absolute plate velocity in cm/yr (Solomon *et al.*, 1975; Richardson *et al.*, 1976). Taking $\sigma_R \simeq 200$ bar (Morgan, 1972; Artyushkov, 1973) and $v \simeq 8$ cm/yr for oceanic plates (Solomon *et al.*, 1975) gives $2 < \tau < 20$ bar.

Given the shear stress and an estimate of the strain rate, the compilation by Kohlstedt and Goetze (1974) of creep measurements in dry olivine may be used to estimate the temperature at the base of the lithosphere. The strain rate ϵ depends on the thickness of the shear zone beneath the lithosphere but is unlikely to exceed 3×10^{-14} sec^{-1}. An extrapolation of the Kohlstedt-Goetze creep relations to lower strain rates than measured (ignoring pressure effects) gives $T = 1100° \pm 100°C$ for $\tau = 2$–20 bar and $\epsilon = 3 \times 10^{-14}$ sec^{-1}. The formal error in temperature is based on a fixed constitutive relation and the given stress range and strain rate and so underestimates the total uncertainty, particularly on the low-temperature side. In-

cipient melting will lower the temperature estimate further, but the results of Auten *et al.* (1974) suggest that the reduction may be small.

The shear stress and the viscosity at the top of the asthenosphere thus provide a useful limit on temperature. Though determining these quantities in the earth and relating them to temperature and composition in the laboratory need further work, the temperature at the top of most oceanic asthenosphere must almost certainly be less than 1200°C and perhaps less than 1100°C.

Electrical conductivity

Electrical conductivity is another physical property highly sensitive to temperature. The electrical conductivity of the upper mantle may be estimated by inversion of geomagnetic variation data (Banks, 1969; Parker, 1970), though at present the data are not accurate enough to extract more than averages over depth intervals of several hundred kilometers (Parker, 1970). The inferred average conductivity of 0.1 $\Omega^{-1}m^{-1}$ for the upper 400 km of the mantle implies a temperature of 1800°C if the conductivity–temperature relation for the most electrically resistive olivine is used (Duba *et al.*, 1974). This is only an upper limit on temperature, since the electrical conductivity averages are dominated by the most conductive regions both radially and laterally and the mantle may be more conductive as a function of temperature than olivine. Accounting for a small amount of partial melt, for instance, could lower the temperature estimate substantially (Chan *et al.*, 1973; Waff, 1974).

Q

Seismic attenuation can also be strongly dependent on temperature. In a partially-melted asthenosphere, the temperature sensitivity is due to a dependence on the viscosity of the melt phase (Walsh, 1969; Solomon, 1972). There are no experimental grounds for assigning a temperature on the basis of a determination of Q at depth, but some limits can be placed on the magnitude of the lateral variation of temperature within the asthenosphere from lateral differences in the travel-time delays and attenuation of P and S waves which travel through the asthenosphere. Figure 4 is a map of temperature variations in the North American asthenosphere (after Solomon, 1972), con-

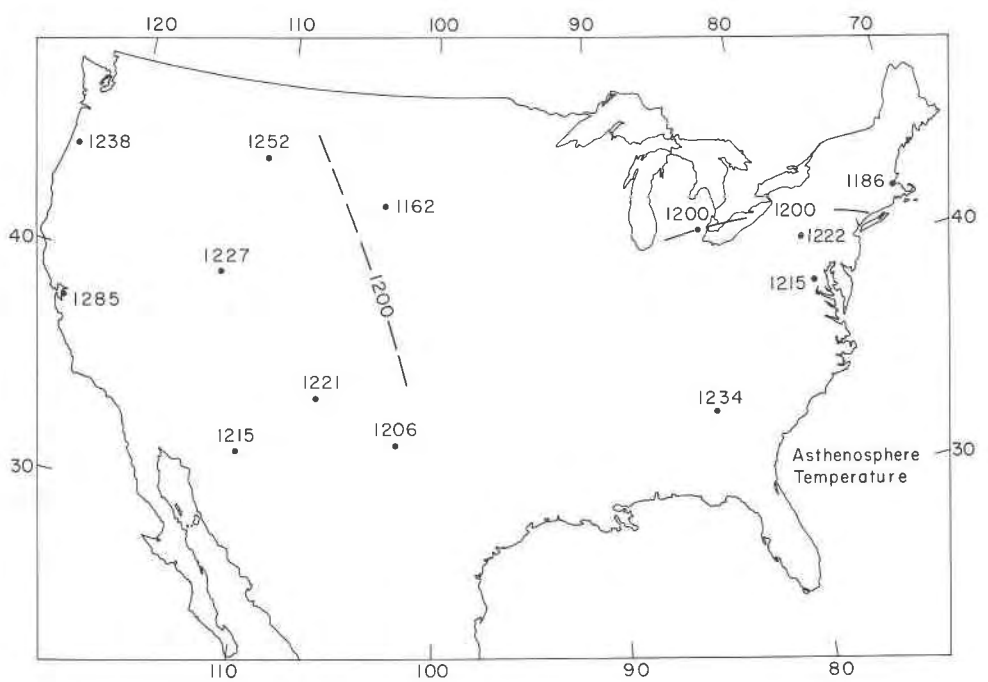

FIG. 4. Lateral variation of temperature (°C) in the asthenosphere of the United States, after Solomon (1972). The value of temperature beneath the point in Michigan is set at 1200°C, and all other values follow from the assumption that seismic-wave travel-time delay and attenuation in the North American asthenosphere are governed by a shear relaxation (Walsh, 1969). The relaxation time is taken to be thermally activated with an activation energy of 57 kcal/mole. Temperatures correspond to a depth in the middle of the low velocity zone, or perhaps 150 km.

structed by assuming that lateral variations in delays and attenuation are due to regional differences in the melt volume and melt viscosity in the asthenosphere. The absolute level of temperature in the asthenosphere is uncertain using these data, but lateral differences of no more than 100° to 200°C are adequate to produce viscosity variations large enough to account for the observed lateral variations in seismic properties.

Phase boundaries as geothermometers: olivine–spinel

Several seismic discontinuities deeper in the mantle have been associated with particular mineralogical phase transitions (Ringwood, 1970), most notably the transition from the olivine to the spinel to the β phase of $(Mg,Fe)_2SiO_4$ (Ringwood and Major, 1970) at about 350 to 400 km depth, and the breakdown of the spinel phase to constituent oxides (Kumazawa *et al.*, 1974; Ming and Bassett, 1975) at about 650 km. If the loci of these boundaries in temperature-pressure-composition space are known from laboratory experiments, then the depth of each such seismic discontinuity may be converted to a temperature in the mantle at that depth (Anderson, 1967). As a check on such determinations, the vertical gradient in seismic velocity, if sufficiently well known, may be compared with velocity profiles predicted from assumed mineralogical assemblages and geotherms passing through the points indicated by phase boundaries (Anderson, 1967; Graham, 1970; Forsyth and Press, 1971).

The 350 km discontinuity

The depths to the top of the olivine–spinel transition as determined by several long refraction profiles are given in Figure 5. The principal uncertainty in locating the transition comes from a possible tradeoff between transition depth and the average velocity in the overlying mantle. Thus, much of the spread in reported depths to the olivine–spinel transition is not real. The three profiles reporting the shallowest transition depth (Massé *et al.*, 1972; Massé, 1973; Simpson *et al.*, 1974), which all have an additional discontinuity 40 to 100 km below the first, were made in regions of pronounced lateral heterogeneity, and thus the spherically symmetric models fit to the profiles are suspect (Julian, 1970). The two deepest reported transitions are from models HWA and HWB of Wiggins and Helmberger (1973), since supplanted by

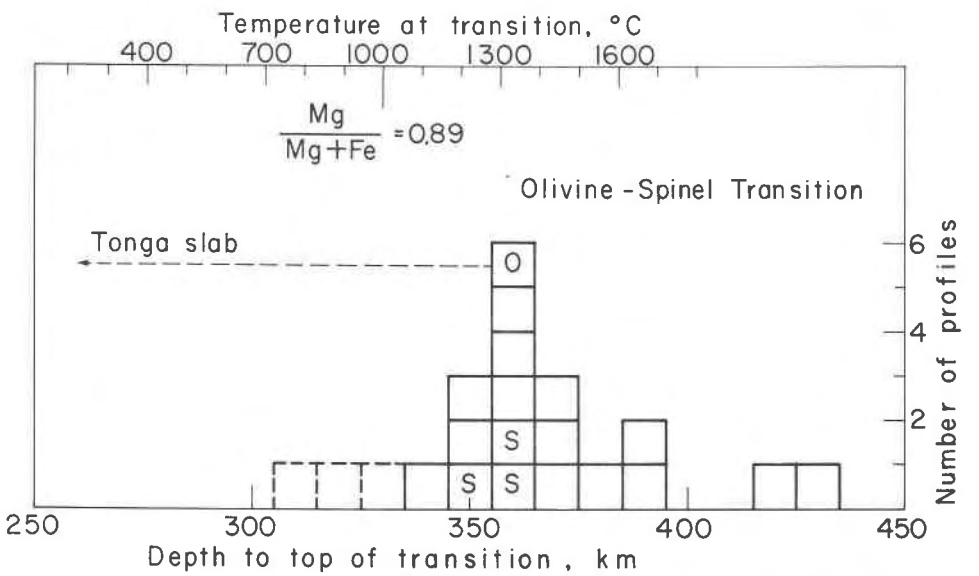

FIG. 5. Seismic determinations of the depth to the top of the olivine–spinel transition. Each box represents the thickness determined from one refraction profile; an *S* within the box designates an *S*-wave profile and the *O* designates the single oceanic determination (Frohlich *et al.*, 1975). Continental profiles include CIT204 (Johnson, 1967), CIT109 through 112 (Archambeau *et al.*, 1969), STAN3 (Kovach and Robinson, 1969), US26 (Anderson and Julian, 1969), HUDSBY 10, YUKON 4, NTS N3, NTS NE1, and NTS E1 (Julian, 1970), SDL-UT-BR1 (dashed, Massé (1972), HWA and HWB (Wiggins and Helmberger, 1973), the Early Rise model (dashed) of Massé (1973), SHR 14 (Helmberger and Engen, 1974), and SMAK1 (dashed, Simpson *et al.*, 1974). Dashed boxes are from profiles crossing pronounced lateral heterogeneities. The conversion from depth (bottom scale) to temperature (top scale) follows Ringwood and Major (1970). The phase change elevation in the Tonga slab is from Fig. 6.

SHR14 of Helmberger and Engen (1974), in which an additional discontinuity of about 500 km depth lies between those at 360 and 620 km.

Excepting the outlier determinations, the olivine–spinel transition appears to lie at 360 ± 10 km depth. This depth may be converted to a temperature at that depth using Ringwood and Major's (1970) experimental high-pressure phase diagram for $(Mg,Fe)_2SiO_4$ at 1000°C, a Clapeyron slope for the reaction of 30 bar/°C, and an Mg/(Mg + Fe) molar fraction for the upper mantle of 0.89 (Ringwood and Major, 1970). At 1000°C the transition occurs at 100 kbar pressure, so at 360 km depth the transition temperature is 1300 ± 150°C. The uncertainty in temperature is calculated assuming a 10 km uncertainty in transition depth, a 0.03 uncertainty in Mg/(Mg + Fe), and a 10 bar/°C uncertainty in the Clapeyron slope. Anderson (1967) and Graham (1970) obtained slightly higher temperatures using somewhat different data.

Some of the variation in the apparent depth to the olivine–spinel transition between neighboring continental profiles may be real (Julian, 1970). Variations of 10 to 30 km in depth would require lateral temperature differences of 100° to 300°C or differences in Mg/(Mg + Fe) of 0.03 to 0.10 (Ringwood and Major, 1970).

The most pronounced lateral temperature variations in the upper mantle occur near subduction zones, and thermal models for the descending plate predict that the olivine–spinel transition will be greatly elevated within the cool slab relative to normal mantle (*e.g.*, Turcotte and Schubert, 1971). This has been verified using the travel times of waves which have propagated through the slab (Fig. 6, after Solomon and Paw U, 1975). The change in the mean *P* wave travel-time residuals with earthquake depth for deep Tonga events observed at Australian stations is more pronounced between about 250 and 350 km depth than over other depth intervals (Fig. 6). This observation requires a higher velocity contrast between slab and normal mantle over that depth range than over other similar intervals, and is most plausibly explained as due to an elevation by 100 km of the olivine–spinel transition in the slab (Solomon and Paw U, 1975). Such an elevation implies a 1000°C temperature contrast between slab and normal mantle at about 250 km depth.

The 650 km discontinuity

For completeness, the several seismic determinations of the depth to the inferred spinel–oxides transition are summarized in Figure 7. Determinations from long refraction profiles and from *P'P'* (*PKPPKP*) precursor times are both included. The latter set of determinations are on the whole the more

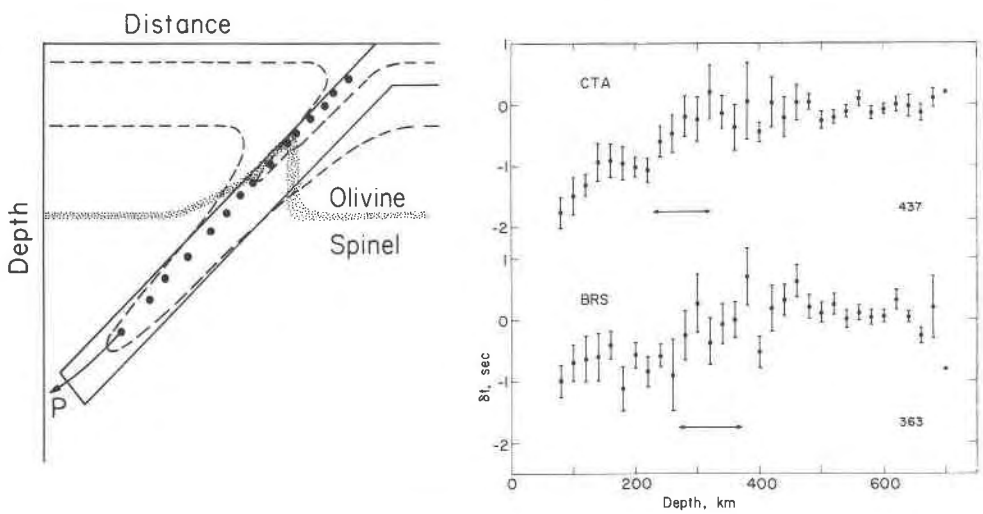

FIG. 6. (Left) A schematic view of the experiment used to detect an elevation of the olivine–spinel phase change in subducted lithosphere. Isotherms (dashed), the phase transition region (shaded), earthquake hypocenters (dots), and a typical *P*-wave path are illustrated. (Right) Mean travel time residual versus earthquake depth for Tonga earthquakes recorded by Australian stations at Charters Towers (CTA) and Brisbane (BRS), from Solomon and Paw U (1975). The arrows delimit approximately the depth interval over which the residual versus depth curves change most rapidly.

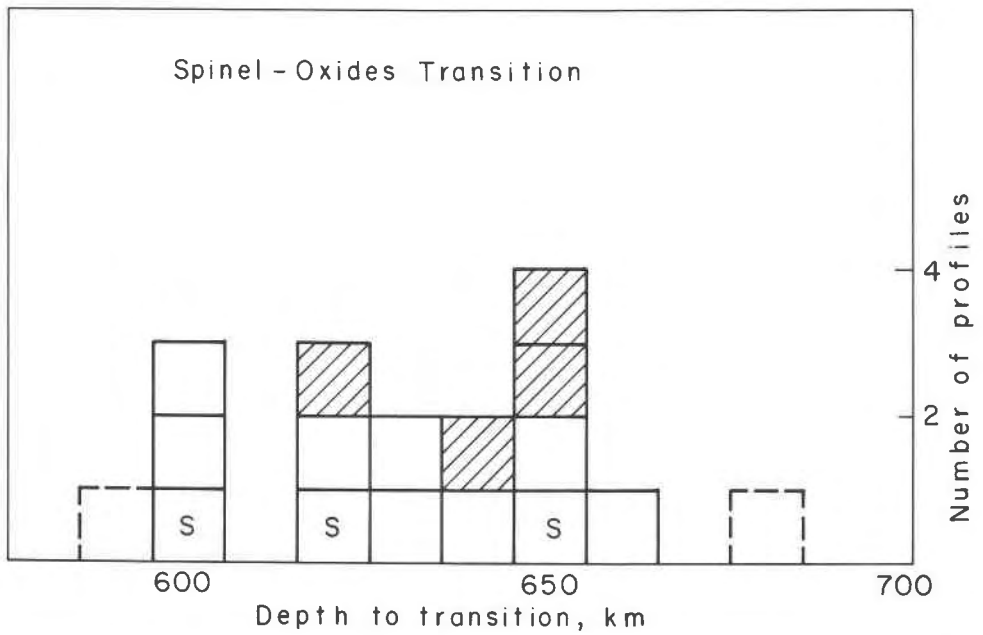

FIG. 7. Seismic determinations of the depth to the inferred spinel–oxides transition. Each box represents one determination. Shaded boxes are estimates using *P'P'* precursors (Engdahl and Flinn, 1969; Whitcomb and Anderson, 1970; Adams, 1971), open boxes (*S* for *S* waves) are from refraction profiles, including CIT204 (Johnson, 1967), CIT109 through 112 (Archambeau *et al.*, 1969), STAN3 (Kovach and Robinson, 1969), US26 (Anderson and Julian, 1969), HWA and HWB (Wiggins and Helmberger, 1973), the NTS east model (dashed) of Massé (1974), SHR14 (Helmberger and Engen, 1974) and SMAK1 (dashed, Simpson *et al.*, 1974).

reliable, since the former depend on the integrated errors in the vertical travel time through the overlying layers; however, the *P'P'* precursors are reflections off a sharp velocity change confined to a depth interval less than 4 km thick (Richards, 1972) and need not mark the top of the transition zone.

The depth to the spinel–oxides transition cannot yet be converted reliably to a temperature, since the dependence of transition pressure on temperature is not known. Even the sign of the Clapeyron slope is uncertain (Jackson *et al.*, 1974). Whether the spread in transition depths has any reality is not yet demonstrable. Fitch (1975) reported higher than normal *P*-wave velocities at about 600 km depth within the Tonga slab, perhaps indicating upward displacement of the 650-km transition. Solomon and Paw U (1975) found no evidence for such a displacement but were not able to rule it out.

Synthesis and discussion

All of the constraints on temperature introduced above may be combined to discuss some of the features of geotherms. A simple but important caution is that there is no single geotherm with any physical reality, nor even meaningful "oceanic" or "continental"[5] geotherms. In oceans, it is clear that the lithospheric portion of the geotherm evolves with lithosphere age. In continents, it appears that the lithospheric limb of the geotherm varies (more slowly) with the age of the upper crust.

Neither will a single geotherm in the asthenosphere be adequate for either oceans or continents. According to the arguments of Richter (1973), Richter and Parsons (1975) and McKenzie and Weiss (1975), heat is transported through the asthenosphere by a convection pattern secondary to the pattern of plate motions. The secondary convection has a horizontal scale comparable to the depth extent of this secondary flow, probably about 600 km. Though the "mean" temperature profile in the asthenosphere will be very nearly adiabatic (McKenzie *et al.*, 1974), the geotherm in any given location will depend on whether the region is over an upwelling, mid-cell, or downwelling portion of the secondary flow and will not necessarily be stationary in time.

Some schematic geotherms

Several oceanic geotherms consistent with the discussion above are sketched in Figure 8. The material upwelling beneath spreading centers will rise more or

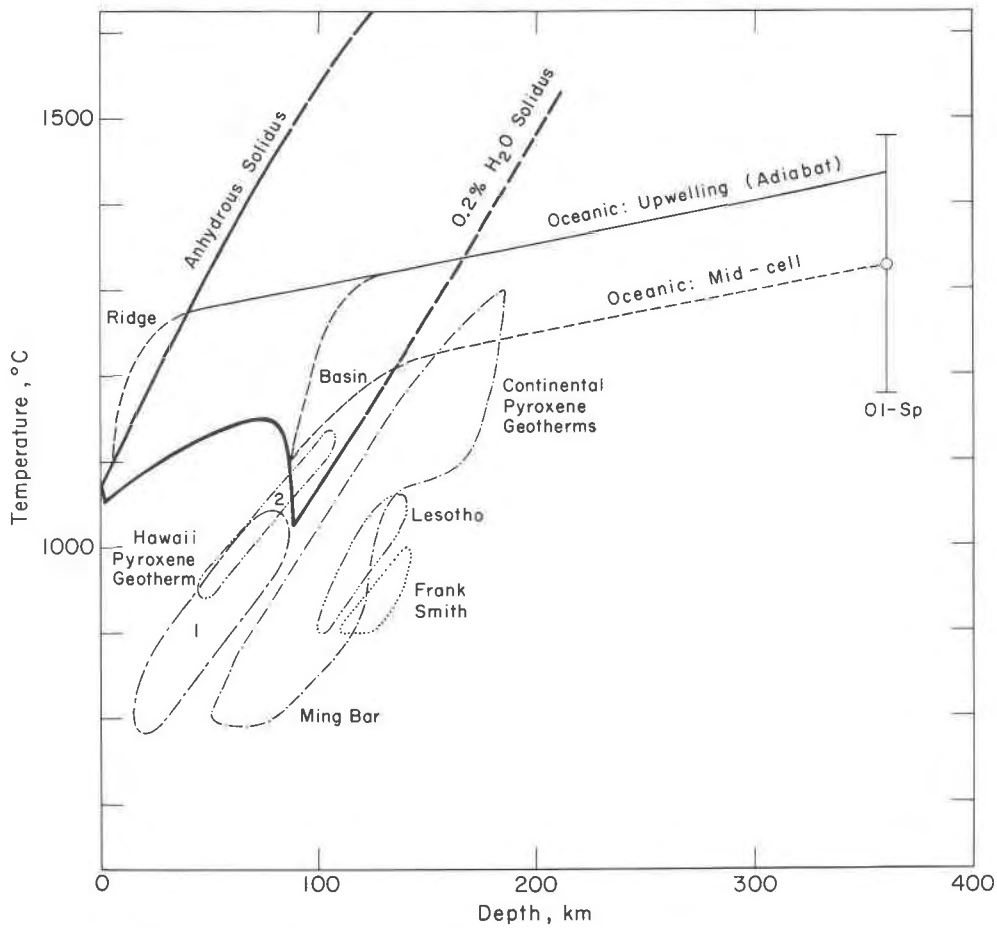

FIG. 8. Some schematic geotherms. The pyrolite solidus with 0.2 percent H_2O and for anhydrous conditions are from Green (1973b). The oceanic upwelling-ridge curve intersects the anhydrous solidus at the depths indicated in Fig. 3 and follows an adiabat below. The oceanic mid-cell curve follows an adiabat upward from the olivine–spinel transition at 360 km depth (Fig. 5) and intersects the solidus at 1100°C and 85 km depth. A curve for upwelling beneath a basin (Hawaii?) is also sketched. Several pyroxene geotherms are included. Hawaiian geotherms 1 and 2 are respectively from MacGregor and Basu (1974) and Mercier and Carter (1975). Geotherms are shown for the Lesotho kimberlite (Boyd and Nixon, 1973), the Frank Smith kimberlite (Boyd, 1974), and the Ming Bar diatreme (Eggler and McCallum, 1974), and approximately bracket other continental geotherms.

less adiabatically from some depth in the lower portion of the asthenosphere. To satisfy Figure 3, the oceanic upwelling-ridge geotherm is drawn to intersect Green's (1973b) anhydrous solidus at 40 and 5 km depth and follows an adiabat below 40 km.

Upwelling associated with the secondary scale of convection (Richter, 1973; Richter and Parsons, 1975; McKenzie and Weiss, 1975) will also occur under ocean basins. An oceanic upwelling-basin geotherm following the same adiabat as the ridge curve has also been sketched. A thermal boundary layer of uncertain thickness separates the adiabatic portion of the curve from the base of the lithosphere, drawn to intersect Green's (1973b) pyrolite + 0.2 percent H_2O solidus at 1100°C (after Fig. 3).

Ocean basin regions situated over downwelling or mid-cell portions of the secondary scale of convection will be characterized by a cooler geotherm below the lithosphere. A oceanic mid-cell-basin geotherm is sketched in Figure 8 to follow an adiabat upward from the olivine–spinel transition at 360 km depth (Fig. 5) and to intersect Green's (1973b) pyrolite + 0.2 percent H_2O solidus at 1100°C. The thermal boundary layer between the lithosphere and that portion of the geotherm with an adiabatic gradient may be thicker than the boundary layer over an upwelling

adiabat, and the mid-cell gradient may actually be subadiabatic in the asthenosphere (McKenzie *et al.*, 1974) The oceanic upwelling and mid-cell geotherms are separated in Figure 8 by about 100°C, an acceptable value (McKenzie *et al.*, 1974) but one for which no independent information is available. The upwelling, mid-cell, and downwelling (not shown) oceanic geotherms meet at the bottom of a second thermal boundary layer located at the base of the secondary flow.

Two pyroxene geotherms based on spinel lherzolite xenoliths in Hawaiian alkali basalts (MacGregor and Basu, 1974; Mercier and Carter, 1975) are also included in Figure 8 and are adequate continuations into the lithosphere of the basin geotherms sketched in the asthenospheric portion of the figure.

An interesting aside is that if a stable basin region sits atop a convective upwelling in the asthenosphere, there is no reason why the geotherm cannot be steeper in the thermal boundary layer at the top of the asthenosphere than in the overlying lithosphere. This would give rise to a "kinked" geotherm such as those reported for South African kimberlites (Boyd, 1973, 1974; Boyd and Nixon, 1973; MacGregor and Basu, 1974). As pointed out by many authors, such a kink cannot be a steady-state feature. If the kink arises as in Figure 8, neither the flow pattern in the asthenosphere (Richter, 1973; McKenzie *et al.*, 1974) nor the relative position of the asthenosphere flow and the overlying lithosphere need be stationary for times comparable to the thermal equilibration time of the lithosphere (~50 m.y.).

Continent-ocean differences

It is now well known that continental and oceanic mantle must differ in temperature and/or in composition at least to depths of about 200 km. The evidence supporting this view includes the following: The mantle contribution to observed surface heat flow appears to differ markedly between stable ocean basins and continental shields (Sclater and Francheteau, 1970), although this difference may be reduced somewhat if corrections are made to the continental measurements to account for different degrees of saturation between *in situ* conditions and laboratory conditions during conductivity determinations (Simmons and Nur, 1968) and for possible paleoclimatological effects (*e.g.*, Horai, 1969). The depth to the low-velocity zone beneath stable continents is greater than beneath ocean basins (Figs. 1 and 2). Finally, pyroxene geotherms determined in continental regions are typically cooler than those for oceanic environments to at least 150 km depth (MacGregor and Basu, 1974). Several continental pyroxene geotherms are shown in Figure 8, including those from the Lesotho (Boyd and Nixon, 1973) and Frank Smith (Boyd, 1974) kimberlites in South Africa and the Ming Bar diatreme in Montana (Eggler and McCallum, 1974). The data of Hearn and Boyd (1973) from Montana plot within or slightly above the field for Ming Bar. The South African kimberlite data of MacGregor and Basu (1974), after shifting to 10 to 15 percent lower pressures as a geobarometer correction, plot in the range of Boyd's kimberlite geotherms.

In a recent provocative paper, Jordan (1975) has argued that thermal and/or compositional differences between ocean basins and continental shields must persist well below 200 km, to at least 400 km depth and probably greater. Jordan offered three main arguments: (1) The *ScS* travel times from deep earthquakes to oceanic island stations are 5 sec later than the times to typical continental stations (Sipkin and Jordan, 1975). This observation, together with measured differences in the phase velocities of long-period surface waves between continental and oceanic paths, requires that systematic differences in *S* wave velocity between oceans and continents extend to at least 400 km depth. (2) The *S* wave travel times through the upper mantle computed from earth models obtained by inversion of free-oscillation periods are several seconds greater than those obtained using body-wave travel times, most commonly recorded at continental stations. Since free oscillations sample a predominantly oceanic earth, Jordan's inference is again that the oceanic and continental structural differences must be deep. (3) Direct examination of the constraints on temperature at depth beneath continents and oceans leads to the conclusion that oceanic and shield geotherms do not intersect above 400 to 600 km.

Each of these arguments, however, can be shown to be inconclusive. Okal and Anderson (1975), using multiple *ScS* arrival times, have shown that the vertical *S*-wave travel time is generally similar beneath old oceanic and old continental regions, clearly implying that the island stations used by Sipkin and Jordan (1975) do not overlie typical oceanic structure. Moreover, differences in the oceanic and continental dispersion curves for long-period surface waves do not by themselves require differences between oceanic and continental structure below 200 km (Dziewonski, 1971).

The difference in the vertical *S*-wave travel time in

the upper mantle between free-oscillation models and body-wave refraction models need not imply deep ocean–continent heterogeneity. An equally plausible explanation, one expected on the basis both of solid-state theory and of attenuation data, is that the greater travel time inferred from the longer-period free-oscillation data arises from a mild frequency dependence of the shear modulus in the upper mantle due to a thermally-activated relaxation process such as incipient melting or viscous grain-boundary relaxation (Nur, 1971; Solomon, 1972).

Jordan's (1975) third argument is based entirely on his particular choice of oceanic and continental geotherms. His conclusion that the thermal contrast between shields and oceans must persist to 400 km arose from selecting an oceanic geotherm too hot by 100 to 200°C (see Figs. 3 and 8) and from basing his shield geotherm on the MacGregor and Basu (1974) pryoxene geotherms, for which the authors admitted a 10 to 15 percent overestimate of pressures.

A more likely comparison of oceanic and continental geotherms is given in Figure 8. The continental regions are cooler than the ocean basins to depths of 150 to 200 km, and the shield geotherms may not intersect the mantle solidus at any depth. Systematic continent–ocean differences do not appear to extend below about 200 km on the basis of any of the thermal arguments considered in this paper. If the asthenosphere below 200 km is indistinguishable beneath oceans and continents then many of Jordan's (1975) other deductions on chemical layering in the mantle and on mantle convection are incorrect.

Conclusions

There is a wide variety of geophysical and mineralogical data that loosely or tightly constrain the temperatures in the earth's upper mantle. Seismological geothermometers include the depth to the top of the low-velocity zone, interpreted as the onset of incipient melting, the depth to the melt-fraction boundary associated with the anhydrous solidus, and the depth to the top of the olivine–spinel transition. Other constraints include the temperatures of erupting lavas, the parameters of lithosphere cooling models, and the measurement of thermally-activated properties of the mantle such as viscosity, electrical conductivity, and seismic attentuation. Pyroxene geothermometry provides results entirely consistent with all the other constraints and may eventually prove to be the temperature-sensing technique with the best depth resolution.

The most probable value for the temperature at the base of the lithosphere, as defined seismically, is $1100° \pm 100°$C on the basis of all considerations. The lithosphere is 90 to 100 km thick beneath old oceans and 50 or more km thicker beneath shields. Shields are about 100° to 200°C cooler than ocean basins at 100 km depth, but the thermal contrast between stable continental and oceanic regions probably disappears by 200 km depth. Thermal gradients throughout most of the asthenosphere are nearly adiabatic. Lateral temperature variations of up to perhaps 200°C persist at least to 400 to 600 km depth and are closely related to the convective flow pattern in the asthenosphere. A major unsolved problem is to relate quantitatively the inferred temperature variations in the asthenosphere to a realizable flow model.

Acknowledgments

I thank Buzz Graham for a critical review and Art Boettcher and Peter Wyllie for instructive discussion. This research has been supported by the Earth Sciences Section, National Science Foundation, NSF Grant DES75-14812, and by the Advanced Research Projects Agency, monitored by the Air Force Office of Scientific Research under contract F44620-75C-0064.

References

ADAMS, R. D. (1971) Reflections from discontinuities beneath Antarctica. *Bull. Seism. Soc. Am.* **61,** 1441–1451.

ALEXANDER, S. S. AND R. W. SHERBURNE (1972) Crust-mantle structure of shields and their role in global tectonics (abstr.). *Eos Trans. Am. Geophys. Un.* **63,** 1043.

ANDERSON, D. L. (1967) Phase changes in the upper mantle. *Science,* **157,** 1165–1173.

——— AND B. R. JULIAN (1969) Shear velocities and elastic parameters of the mantle. *J. Geophys. Res.* **74,** 3281–3286.

——— AND C. SAMMIS (1970) Partial melting and the low-velocity zone. *Phys. Earth Planet. Int.* **3,** 41–50.

ARCHAMBEAU, C. B., E. A. FLINN AND D. G. LAMBERT (1969) Fine structure of the upper mantle. *J. Geophys. Res.* **74,** 5825–5865.

ARTYUSHKOV, E. V. (1973) Stresses in the lithosphere caused by crustal thickness inhomogeneities. *J. Geophys. Res.* **78,** 7675–7708.

ASADA, T. AND H. SHIMAMURA (1975) A structure of the oceanic lithosphere as revealed by ocean-bottom seismography (abstr). *Abstracts of Papers Presented at the Interdisciplinary Symposia, XVI General Assembly, I.U.G.G., Grenoble,* p. 91.

AULT, W. V., J. P. EATON AND D. H. RICHTER (1961) Lava temperatures in the 1959 Kilauea eruption and cooling lake. *Geol. Soc. Am. Bull.* **72,** 791–794.

AUTEN, T. A., R. B. GORDON AND R. L. STOCKER (1974) Q and mantle creep. *Nature,* **250,** 317–318.

BANKS, R. J. (1969) Geomagnetic variations and the electrical conductivity of the upper mantle. *Geophys. J. R. Astron. Soc.* **17,** 457–487.

BISWAS, N. N. AND L. KNOPOFF (1974) The structure of the upper mantle under the United States from the dispersion of Rayleigh waves. *Geophys. J. R. Astron. Soc.* **36,** 515–539.

BOETTCHER, A. L. (1974) Review of symposium on deep-seated rocks and geothermometry. *Eos Trans. Am. Geophys. Un.* **55,** 1068–1072.

BOYD, F. R. (1973) A pyroxene geotherm. *Geochim. Cosmochim. Acta*, **37**, 2533–2546.

——— (1974) Ultramafic nodules from the Frank Smith kimberlite pipe, South Africa. *Carnegie Inst. Wash. Year Book*, **73**, 285–294.

——— AND P. H. NIXON (1973) Structure of the upper mantle beneath Lesotho. *Carnegie Inst. Wash. Year Book*, **72**, 431–445.

BRUNE, J. AND J. DORMAN (1963) Seismic waves and earth structure in the Canadian shield. *Bull. Seism. Soc. Am.* **53**, 167–210.

BULTITUDE, R. J. AND D. H. GREEN (1967) Experimental study at high pressures on the origin of olivine nephelinite and olivine melilite nephelinite magmas. *Earth Planet. Sci. Lett.* **3**, 325–337.

CHAN, T., E. NYLAND AND D. I. GOUGH (1973) Partial melting and conductivity anomalies in the upper mantle. *Nature Phys. Sci.* **244**, 89–91.

DUBA, A., H. C. HEARD AND R. N. SCHOCK (1974) Electrical conductivity of olivine at high pressure and under controlled oxygen fugacity. *J. Geophys. Res.* **79**, 1667–1673.

DZIEWONSKI, A. M. (1971) Upper mantle models from "pure path" dispersion data. *J. Geophys. Res.* **76**, 2587–2601.

EATON, J. P. AND K. J. MURATA (1960) How volcanoes grow. *Science*, **132**, 925–938.

EGGLER, D. H. AND M. E. MCCALLUM (1974) Xenoliths in diatremes of the western United States. *Carnegie Inst. Wash. Year Book*, **73**, 294–300.

ENGDAHL, E. R. AND E. A. FLINN (1969) Seismic waves reflected from discontinuities within earth's upper mantle. *Science*, **163**, 177–179.

FITCH, T. J. (1975) Compressional velocity in source regions of deep earthquakes: an application of the master earthquake technique. *Earth Planet. Sci. Lett.* **26**, 156–166.

FORSYTH, D. W. (1975) The early structural evolution and anisotropy of the oceanic upper mantle. *Geophys. J. R. Astron. Soc.* **43**, 103–162.

——— AND F. PRESS (1971) Geophysical tests of petrological models of the spreading lithosphere. *J. Geophys. Res.* **76**, 7963–7979.

FRANCIS, T. J. G. AND I. T. PORTER (1973) Median valley seismology: the mid-Atlantic ridge near 45°N. *Geophys. J. R. Astron. Soc.* **34**, 279–311.

FREY, F. A., W. B. BRYAN AND G. THOMPSON (1974) Atlantic Ocean floor: geochemistry and petrology of basalts from legs 2 and 3 of the Deep-Sea Drilling Project. *J. Geophys. Res.* **79**, 5507–5527.

FROHLICH, C., M. BARAZANGI AND B. L. ISACKS (1975) The upper mantle beneath the Fiji basin: seismic observations of second *P* arrivals from the 400 kilometer transition zone (abstr.). *Eos Trans. Am. Geophys. Un.* **56**, 393.

GRAHAM, E. K. (1970) Elasticity and composition of the upper mantle. *Geophys. J. R. Astron. Soc.* **20**, 285–302.

GREEN, D. H. (1971) Composition of basaltic magmas as indicators of condition of origin: application to oceanic volcanism. *Phil. Trans. R. Soc. Lond.* A **268**, 707–725.

——— (1973a) Conditions of melting of basanite magma from garnet peridotite. *Earth Planet. Sci. Lett.* **17**, 456–465.

——— (1973b) Experimental melting studies on a model upper mantle composition at high pressure under water-saturated and water-undersaturated conditions. *Earth Planet. Sci. Lett.* **19**, 37–53.

GREEN, H. W., II (1972) A CO_2 charged asthenosphere, *Nature Phys. Sci.* **238**, 2–5.

GREEN, R. W. E. AND A. L. HALES (1968) The travel times of *P* waves to 30° in the central United States and upper mantle structure. *Bull. Seism. Soc. Am.* **58**, 267–289.

HEARN, B. C., JR. AND F. R. BOYD (1973) Garnet peridotite xenoliths in a Montana, U.S.A., kimberlite (abstr.). *International Conference on Kimberlites*, Extended Abstracts of Papers, Capetown, South Africa, 167–169.

HELMBERGER, D. V. AND G. R. ENGEN (1974) Upper mantle shear structure. *J. Geophys. Res.* **79**, 4017–4028.

HOLLAND, H. D. (1962) Model for the evolution of the earth's atmosphere. In, A. E. G. Engel, H. L. James, and B. F. Leonard, Eds., *Petrologic Studies: A Volume in Honor of A. F. Buddington.* Geol. Soc. Am., New York p. 447–477.

HORAI, K. (1969) Effect of past climatic changes on the thermal field of the earth. *Earth Planet. Sci. Lett.* **6**, 39–42.

IRVING, A. J. AND P. J. WYLLIE (1973) Melting relationships in $CaO–CO_2$ and $MgO–CO_2$ to 36 kilobars with comments on CO_2 in the mantle. *Earth Planet. Sci. Lett.* **20**, 220–225.

JACKSON, I. N. S., R. C. LIEBERMANN AND A. E. RINGWOOD (1974) Disproportionation of spinels to mixed oxides: significance of cation configuration and implications for the mantle. *Earth Planet. Sci. Lett.* **24**, 203–208.

JOHNSON, L. R. (1967) Array measurements of *P* velocities in the upper mantle. *J. Geophys. Res.* **72**, 6309–6325.

JORDAN, T. H. (1975) The continental tectosphere. *Rev. Geophys. Space Phys.* **13**, 1–12.

JULIAN, B. R. (1970) *Regional variations in upper mantle structure beneath North America.* Ph.D. Thesis, California Institute of Technology, Pasadena, California.

KAY, R., N. J. HUBBARD AND P. W. GAST (1970) Chemical characteristics and origin of oceanic ridge volcanic rocks. *J. Geophys. Res.* **75**, 1585–1613.

KINOSHITA, W. T., R. Y. KOYANAGI, T. L. WRIGHT AND R. S. FISKE (1969) Kilauea volcano: the 1967–68 summit eruption. *Science*, **166**, 459–468.

KNOPOFF, L. (1972) Observation and inversion of surface-wave dispersion. *Tectonophysics*, **13**, 497–519.

KOHLSTEDT, D. L. AND C. GOETZE (1974) Low-stress high-temperature creep in olivine single crystals. *J. Geophys. Res.* **79**, 2045–2051.

KOVACH, R. L. AND R. ROBINSON (1969) Upper mantle structure in the Basin and Range province, western North America, from the apparent velocities of *S* waves. *Bull. Seism. Soc. Am.* **59**, 1653–1665.

KUDO, A. M. AND D. F. WEILL (1970) An igneous plagioclase thermometer. *Contrib. Mineral. Petrol.* **25**, 52–65.

KUMAZAWA, M., H. SAWAMOTO, E. OHTANI AND K. MASAKI (1974) Post-spinel phase of forsterite and evolution of the earth's mantle. *Nature*, **247**, 356–358.

KUSHIRO, I., Y. SYONO AND S. AKIMOTO (1967) Stability of phlogopite at high pressures and possible presence of phlogopite in the earth's upper mantle. *Earth Planet. Sci. Lett.* **3**, 197–203.

———, ——— AND ——— (1968) Melting of a peridotite nodule at high pressures and high water pressures. *J. Geophys. Res.* **73**, 6023–6029.

LAMBERT, I. B. AND P. J. WYLLIE (1968) Stability of hornblende and a model for the low velocity zone. *Nature*, **219**, 1240–1241.

LEE, W. B. AND S. C. SOLOMON (1975) Inversion schemes for surface wave attenuation and *Q* in the crust and the mantle. *Geophys. J. R. Astron. Soc.* **43**, 47–71.

LEEDS, A. R. (1975) Lithospheric thickness in the western Pacific. *Phys. Earth Planet. Int.* **11**, 61–64.

———, L. KNOPOFF AND E. G. KAUSEL (1974) Variations of upper mantle structure under the Pacific Ocean. *Science*, **186**, 141–143.

MACGREGOR, I. D. (1974) The system $MgO–Al_2O_3–SiO_2$: solubil-

ity of Al_2O_3 in enstatite for spinel and garnet peridotite compositions. *Am. Mineral.* **59,** 110–119.

——— AND A. R. BASU (1974) Thermal structure of the lithosphere: a petrologic model. *Science,* **185,** 1007–1011.

MASSÉ, R. P. (1973) Compressional velocity distribution beneath central and eastern North America. *Bull. Seism. Soc. Am.* **63,** 911–935.

——— (1974) Compressional velocity distribution beneath central and eastern North America in the depth range 450–800 km. *Geophys. J. Roy. Astron. Soc.* **36,** 705–716.

———, M. LANDISMAN AND J. B. JENKINS (1972) An investigation of the upper mantle compressional velocity distribution beneath the Basin and Range province. *Geophys. J. R. Astron. Soc.* **30,** 19–36.

MATHEZ, E. A. (1973) Refinement of the Kudo-Weill plagioclase thermometer and its application to basaltic rocks. *Contrib. Mineral. Petrol.* **41,** 61–72.

MCGETCHIN, T. R. AND L. T. SILVER (1972) A crustal-upper mantle model for the Colorado plateau based on observations of crystalline rock fragments in the Moses Rock dike. *J. Geophys. Res.* **77,** 7022–7037.

———, ——— AND A. A. CHODOS (1970) Titanoclinohumite: a possible mineralogical site for water in the upper mantle. *J. Geophys. Res.* **75,** 255–259.

MCKENZIE, D. P. (1967) Some remarks on heat flow and gravity anomalies. *J. Geophys. Res.* **72,** 6261–6273.

———, J. M. ROBERTS AND N. O. WEISS (1974) Convection in the earth's mantle: towards a numerical simulation. *J. Fluid Mech.* **62,** 465–538.

——— AND N. O. WEISS (1975) Speculations on the thermal and tectonic history of the earth. *Geophys. J. R. Astron. Soc.* **42,** 131–174.

MERCIER, J.-C. AND N. L. CARTER (1975) Pyroxene geotherms. *J. Geophys. Res.* **80,** 3349–3362.

MERRILL, R. B., J. K. ROBERTSON AND P. J. WYLLIE (1972) Dehydration reaction of titanoclinohumite: reconnaissance to 30 kilobars. *Earth Planet. Sci. Lett.* **14,** 259–262.

MILLHOLLEN, G. L., A. J. IRVING AND P. J. WYLLIE (1974) Melting interval of peridotite with 5.7 percent water to 30 kilobars. *J. Geol.* **82,** 575–587.

MING, L. C. AND W. A. BASSETT (1975) The postspinel phases in the Mg_2SiO_4–Fe_2SiO_4 system. *Science,* **187,** 66–68.

MOORE, J. G. (1970) Water content of basalt erupted on the ocean floor. *Contrib. Mineral. Petrol.* **28,** 272–279.

MORGAN, W. J. (1972) Deep mantle convection plumes and plate motion. *Am. Assoc. Petrol. Geol. Bull.* **56,** 203–213.

MYSEN, B. O. AND A. L. BOETTCHER (1975) Melting of a hydrous mantle, 1, phase relations of natural peridotite at high pressures and temperatures with controlled activities of water, carbon dioxide and hydrogen. *J. Petrol.* **16,** 520–548.

NEWTON, R. C. AND W. E. SHARP (1975) Stability of forsterite + CO_2 and its bearing on the role of CO_2 in the mantle. *Earth Planet. Sci. Lett.* **26,** 239–244.

NORDLIE, B. E. (1971) The composition of the magmatic gas of Kilauea and its behavior in the near surface environment. *Am. J. Sci.* **271,** 417–463.

NUR, A. (1971) Viscous phase in rocks and the low-velocity zone. *J. Geophys. Res.* **76,** 1270–1277.

OKAL, E. A. AND D. L. ANDERSON (1975) A study of lateral inhomogeneities in the upper mantle by multiple *ScS* travel-time residuals. *Geophys. Res. Lett.* **2,** 313–316.

ORCUTT, J., B. KENNETT, L. DORMAN AND W. PROTHERO (1975) A low velocity zone underlying a fast-spreading rise crest. *Nature,* **256,** 475–476.

OXBURGH, E. R. (1964) Petrological evidence for the presence of amphibole in the upper mantle and its petrogenetic and geophysical implications. *Geol. Mag.* **101,** 1–19.

PARKER, R. L. (1970) The inverse problem of electrical conductivity in the mantle. *Geophys. J. R. Astron. Soc.* **22,** 121–138.

PARSONS, B. AND J. G. SCLATER (1975) An analysis of the variation of ocean floor heat flow and bathymetry with age. *J. Geophys. Res.*, in press.

PRESS, F. (1959) Some implications on mantle and crustal structure from *G* waves and Love waves. *J. Geophys. Res.* **64,** 565–568.

RICHARDS, P. G. (1972) Seismic waves reflected from velocity gradient anomalies within the earth's upper mantle. *Z. Geophys.* **38,** 517–527.

RICHARDSON, R. M., S. C. SOLOMON AND N. H. SLEEP (1976) Intraplate stress as an indicator of plate tectonic driving forces. *J. Geophys. Res.*, **81,** 1847–1856.

RICHTER, F. M. (1973) Convection and large-scale circulation of the mantle. *J. Geophys. Res.* **78,** 8735–8745.

——— AND B. PARSONS (1975) On the interaction of two scales of convection in the mantle. *J. Geophys. Res.* **80,** 2529–2541.

RINGWOOD, A. E. (1969) Composition and evolution of the upper mantle. In, P. J. Hart, Ed., *The Earth's Crust and Upper Mantle. Am. Geophys. Un. Mon.* **13.** p. 1–17.

——— (1970) Phase transformations and the constitution of the mantle. *Phys. Earth Planet. Int.* **3,** 109–155.

——— AND A. MAJOR (1970) The system Mg_2SiO_4–Fe_2SiO_4 at high pressures and temperatures. *Phys. Earth Planet. Sci.* **3,** 89–108.

ROEDDER, E. (1965) Liquid CO_2 inclusions in olivine bearing nodules and phenocrysts from basalts. *Am. Mineral.* **50,** 1746–1782.

ROEDER, P. L. AND R. F. EMSLIE (1970) Olivine liquid equilibrium. *Contrib. Mineral. Petrol.* **29,** 275–289.

SCHEIDEGGER, K. F. (1973) Temperatures and composition of magmas ascending along mid-ocean ridges. *J. Geophys. Res.* **78,** 3340–3355.

SCLATER, J. G., R. N. ANDERSON AND M. L. BELL (1971) Elevation of ridges and evolution of the central eastern Pacific. *J. Geophys. Res.* **76,** 7888–7915.

——— AND J. FRANCHETEAU (1970) The implications of terrestrial heat flow observations on current tectonic and geochemical models of the crust and upper mantle of the earth. *Geophys. J. R. Astron. Soc.* **20,** 509–542.

SHOEMAKER, E. M., C. H. ROACH AND F. M. BYERS, JR. (1962) Diatremes and uranium deposits in the Hopi Buttes, Arizona. In, A. E. J. Engel, H. L. James, and B. G. Leonard, Eds., *Petrologic Studies: A Volume in Honor of A. F. Buddington.* Geol. Soc. Am., New York. p. 327–355.

SHURBET, D. H. (1972) Low-velocity layer in the upper mantle beneath Mexico. *Geol. Soc. Am. Bull.* **83,** 3475–3478.

SIMMONS, G. AND A. NUR (1968) Granites: relation of properties *in situ* to laboratory measurements. *Science,* **162,** 789–791.

SIMPSON, D. W., R. F. MEREU AND D. W. KING (1974) An array study of *P*-wave velocities in the upper mantle transition zone beneath northeastern Australia. *Bull. Seism. Soc. Am.* **64,** 1757–1788.

SIPKIN, S. A. AND T. H. JORDAN (1975) Lateral heterogeneity of the upper mantle determined from the travel times of *ScS*. *J. Geophys. Res.* **80,** 1474–1484.

SLEEP, N. H. (1969) Sensitivity of heat flow and gravity to the mechanism of sea-floor spreading. *J. Geophys. Res.* **74,** 542–549.

SOLOMON, S. C. (1972) Seismic-wave attenuation and partial melt-

ing in the upper mantle of North America. *J. Geophys. Res.* **77,** 1483–1502.

——— (1973) Shear-wave attenuation and melting beneath the mid-Atlantic ridge. *J. Geophys. Res.* **78,** 6044–6059.

——— AND B. R. JULIAN (1974) Seismic constraints on ocean-ridge mantle structure: anomalous fault-plane solutions from first motions. *Geophys. J. R. Astron. Soc.* **38,** 265–285.

——— AND K. T. PAW U (1975) Elevation of the olivine–spinel transition in subducted lithosphere: seismic evidence. *Phys. Earth Planet. Int.* **11,** 97–108.

———, N. H. SLEEP AND R. M. RICHARDSON (1975) On the forces driving plate tectonics: inferences from absolute plate velocities and intraplate stress. *Geophys. J. R. Astron. Soc.* **42,** 769–802.

SYKES, L. R. AND M. L. SBAR (1973) Intraplate earthquakes, lithospheric stresses and the driving mechanism of plate tectonics. *Nature,* **245,** 298–302.

TILLEY, C. E., R. N. THOMPSON AND P. A. LOVENBURY (1972) Melting relations of some oceanic basalts. *Geol. J.* **8,** 59–64.

TURCOTTE, D. L. AND G. SCHUBERT (1971) Structure of the olivine–spinel phase boundary in the descending lithosphere. *J. Geophys. Res.* **76,** 7980–7987.

WAFF, H. S. (1974) Theoretical considerations of electrical conductivity in a partially molten mantle and implications for geothermometry. *J. Geophys. Res.* **79,** 4003–4010.

WALSH, J. B. (1969) A new analysis of attenuation in partially melted rock. *J. Geophys. Res.* **74,** 4333–4337.

WEIDNER, D. J. (1974) Rayleigh wave phase velocities in the Atlantic Ocean. *Geophys. J. R. Astron. Soc.* **36,** 105–139.

WHITCOMB, J. H. AND D. L. ANDERSON (1970) Reflection of *P'P'* seismic waves from discontinuities in the mantle. *J. Geophys. Res.* **75,** 5714–5728.

WIGGINS, R. A. AND D. V. HELMBERGER (1973) Upper mantle structure of the western United States. *J. Geophys. Res.* **78,** 1869–1880.

WILSHIRE, H. G. AND E. D. JACKSON (1975) Problems in determining mantle geotherms from pyroxene compositions of ultramafic rocks. *J. Geol.* **83,** 313–329.

WYLLIE, P. J. (1971) Role of water in magma generation and initiation of diapiric uprise in the mantle. *J. Geophys. Res.* **76,** 1328–1338.